Punching Shear Behavior of a Glass Fibers Bubble Deck Slab Subjected to Fire and Cooled by Water

Muntadher Kadhim Al-Fwadhil[1], Waleed A. Waryosh[1]

[1]*Civil Engineering Department, college of Engineering, Mustansiriyah University, Baghdad, Iraq*

ABSTRACT : *The purpose of this experiment is to investigate the efficacy of including Glass fiber (polypropylene fiber) in enhancing the characteristics of concrete and punching shear strength of reinforced concrete bubble slabs exposed to elevated temperatures and water cooled. In this investigation, fifteen panels were tested. The models represent the negative bending moment zone surrounding an interior column supporting bubble slabs. One set of slab specimens was evaluated at room temperature, while the other three groups were examined with different cooling methods after being exposed to high temperatures. The test weights were increased incrementally until the maximum carrying capacity was reached. The following parameters were measured: Ultimate punching shear, deflections, crack patterns, angle of failure and critical zone.*

KEYWORDS: *High Temperature, Bubble Slab, Glass Fiber Concrete, Water Cooling, Punching Shear*.

I. INTRODUCTION

Punching shear strength for reinforced concrete (RC) slabs are important not just to cover their service life but, rather often, to rehabilitate them after they have been damaged during special events, for example earthquakes, fires etc.

Exposure to high temperatures is a significant issue for buildings and structures. Concrete, the most extensively used building material, is thermally sensitive. For instance, it is widely recognized that the behavior of concrete under high temperature circumstances is influenced by parameters such as heating rate, peak temperatures, and constituent materials. Thus, in order to assess structural safety following a fire, it is critical to understand the residual mechanical properties of concrete during expose to real fire flame. [1]. According to experimental investigations, the strength and performance of concrete will be diminished at high temperatures due to Micro-structure cracks, as well as changes in concrete volume generated by thermal pressures [2]. The influence related to fire on structural members be governed by different aspects such as the temperature rate, duration and distribution of fire loading as well as cooling method (gradually or suddenly). Also, fire source either standard fire or real fire flame the building's system requires to be designed not only to withstand dead and live loads, but is also designed to withstand fire resistance [3]. Fire resistance associated with reinforced concrete slab is expressed in terms of fire resistance as

determined by the standard fire tests. After fire is brought to the desired intensity, the slab is scheduled to be overcome in a specified time frame. The standard method (ASTM E-119) [4] of floor slab fire tests specifies that if "the temperature rise of the unexposed area is less than 120 ° C, the fire test is considered to be successfully performed. In order to produce this product, regulations have specified that the steel must not be heated to over 540°C in the fire endurance phase. Once the span increases, the amount of deflection also increases. Therefore, the thickness of slabs should be increased. With the added thickness of slab, the roof will be heavier and the foundation thickness and column cross section are both increased. Buildings also consume more materials such as reinforcement steel and concrete.

For the purpose of avoiding such drawbacks, Bubbled Reinforced Concrete Slab System (also referred to as Voided Slab System), was lately used in Europe. It has been developed via Jorgen Breuning (Danish engineer). The system contains hollow plastic spheres cast in concrete for creating grid related to the void forms in slab. RC bubble slab generally consists from bottom reinforcing mesh, plastic balls and top reinforcing mesh. Checking the failure of punching shear and the strength of the slab-column connections is one of the critical analyzes that must be carried out if bubbled slab is to be used. This type of failure occurs at a load path below the flexural capacity as the transverse shear stress concentrates around the

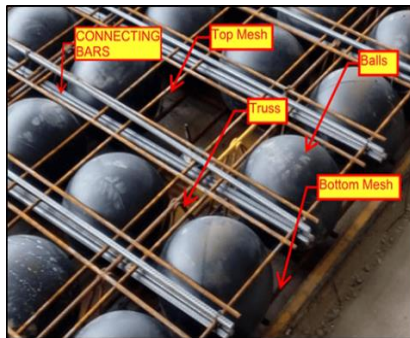column slab connections [5]. Fig.1 indicates a "RC" bubble slab system.

Fig. 1 Demonstrates the RC Bubble Slab System

Shear strength of any concrete slab is mostly affected by the mass of the concrete. Due to the presence of the plastic sphere, the shear resistance of bubbled RC slabs is considerably reduced when compared to solid RC slabs. According to certain theoretical models, the shear strength of bubbled slabs is (70-90%) that of solid slabs with the same depths. Thus, a 0.6 reduction factor will be applied to the shear capacity of all bubbled RC slabs [6].The major rationale for adopting fibers from a structural standpoint is to enhance crack characteristics and structural behavior through the fibers' capacity to bridge cracks. Fiber bridging across cracks increases shear, punching, and moment resistance, decreases crack spacing and widths, increases flexural stiffness, and increases compression ductility.In 2010, Abbas [7] investigated the effect of adding glass fibers to flat plates concrete slabs that had been exposed to elevated temperatures and discovered that glass fibers had a minor improvement effect on ultimate punching shear strength and a significant impact on crack patterns of flat plate slabs even after they had been exposed to high temperatures. Jaber [8] et al in 2021 study experimentally polypropylene fiber effect on the concrete mechanical properties as a material and Behavior and the strength of polypropylene fiber reinforced concrete slab specimens. The experimental results showed a noticeable increase in concrete strength by using polypropylene fiber which also works as crack bridging. The concrete compressive strength could be increased, and the cracks width could be decreased by adding polypropylene fibers to the mixes.

II. EXPERIMENTAL WORK

2.1 Experimental Model

Fifteen RC bubble slabs have been cast in the Structural Engineering Laboratory of College of Engineering at Mustansiriyah University in Baghdad. The examined slabs in this research were all square in shape and modeled as 1/5 of BD230 that mention in (Bubble Deck Span Guide) [9], with dimensions of (500x500) mm and 50 mm thickness and concrete cover was 10 mm. They were supported around their four edges using steel frame and loaded centrally with a square-sectioned steel cube of (40x40x40) mm. Bubble diameter was (30) mm with a spacing between bubbles (40) mm center to center and the reinforcement in both bottom and top layer is $\phi 3$ @ 20 mm (wire mesh). As shown in fig. 2.
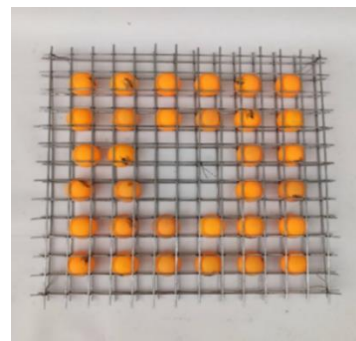

Fig. 2 Steel Reinforcement Mesh with Bubbles

The bubbles were removed from all specimens' punching shear critical sections to meet the punching shear requirements of (Bubble Deck Slab Properties) [6], which underlines the importance of dealing with that area carefully because the bubble that replaced concrete there making the slabs weaker in resistant punching shear force.

2.2 Research Variables

Fifteen specimens were divided into three groups according to its concrete types. First group made of normal strength concrete (NSC) with 30 MPa $f\acute{c}$, second group made of 0.5 % glass fibers concrete (GF-0.5) and third group made of 1.0 % glass fibers concrete (GF-1.0). Each group consist of 5 specimens, reference slab that doesn't burned and 4 slabs burned and cooled in different method which is gradually air cooling and water cooling by three ways; spraying water for 5 minutes, spraying

water for 10 minutes and quenching in water for 10 minutes.

2.3 Materials

All used materials are described in Table 1.

- Cement: Ordinary Portland Cement (Type I).
- Fine aggregate (Sand): Natural sand of (4.75mm) maximum size.
- Coarse aggregate (Gravel): Crushed gravel of (12.5 mm) maximum size.
- Glass Fibers: High-performancemonofilament polypropylene fibers formulated especially for crack control in cementitious materials.
- Plastic Balls: 30 mm dimeter recycled plastic balls
- Reinforcement Mesh: welded mesh was tested in accordance with (A1064/A1064M - 18a) [10].
- Tap water.

All local materials were conforming to applicable standards and specifications.

2.4 Concrete Mix Design

The mix proportions of NSC (30 MPa $f\acute{c}$) used in this study are mentioned in Table (1), based on previous studies [11]. Glass fibers concrete mix design used in this study based on the same mix design of normal strength concrete except for adding glass fibers by two proportion (0.5-1.0) % by volume of plain concrete.

Table 1 Properties of Concrete Mix

Mix notation	NSC
Average Nominal Compressive Strength $f\acute{c}$ (MPa)	30
w/c	0.45
Cement kg/m^3	400
Water (L)	180
Sand kg/m^3	600
Gravel kg/m^3	1200
Glass fiber g/m^3 (in GF-0.5)	5
Glass fiber g/m^3 (in GF-1.0)	10

After that all specimens were casted and curing in the Structural Engineering Laboratory at College of Engineering in Mustansiriyah University. Fig. 3 shows the casted slabs and control specimens.
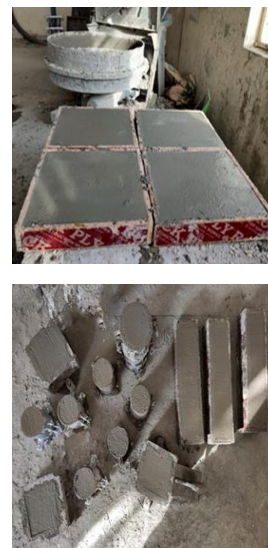

Fig. 3 Bubbled Reinforced Concrete Slabs and control specimens Casting

2.5 Test Procedure

After allowing adequate curing time for the slabs (28 day) (ASTM C31 / C31M-12) [12], All specimens were cleaned and ready for the next step. First phase in testing process is to burn 12 slabs and hold 3 slabs as references for comparison. Following the completion of the burning test, slabs were cooled in 4 methods and subjected to a punching shear load test.

2.6 Burning Slabs

The bubble RC slab specimens were exposed to fire flame by the burners represented in Fig. 4. The fire flame is subjected to tension side of slabs, the distance between slab and fire flame is 20 cm. A steel fire chamber was used to present the true state of burning room; the frame was sealed on all sides with one opening as depicted on the Fig. 5.

Fig. 4 The Burner

Fig. 5 Fire Chamber

An infrared thermometer with a temperature range of (-32 to 550) °C was used to calculate fire intensity on slab's bottom face. The temperature measuring unit is depicted in Fig. 6.

Fig. 6 Infrared Thermometer

The specimens were burnt at a temperature of 300 °C for 30 minutes, with the face exposed to fire being tested every 5 minutes to determine the temperature of concrete and to guarantee that it stayed within the 300 °C cap as shown in Fig. 7. The average temperature on the other face was also measured to determine how heat is transmitted through the concrete.

Fig. 7 Taking Average Temperature for Concrete

2.7 Cooling Slabs

After burning stage of specimens is finished, it is moved to cooling stage, which is in four forms. The first method is to leave the specimens to cool down at room temperature, the second method is to immerse it in water for 10 minutes as in Fig. (8), and the third and fourth methods are to spray the specimens with water for 5 and 10 minutes, respectively as in Fig. (9). The immersion was performed in one of the basins, which is the same temperature as tap water used in spraying which is about 15 °C.

Fig. 8 Quenching Slab in Water

Fig. 9 Spraying Water on Slabs

2.8 Punching Shear Test

The slab was labeled carefully and then they were placed on a rigid support with a clear span of (0.5x0.5) m. The point load was applied at the center of the slab and a 0.01mm dial gauge was positioned directly under the middle of each slab. to measure the central deflection. All slabs were tested using a hydraulic universal testing machine of the type (EPP300MFL system) with a capacity of (3000 kN) available in the structural Laboratory in Civil Engineering Department, College of Engineering, Mustansiriyah University. The load was applied progressively in 2.5 kN increments.

Throughout the test, the number of loads and subsequent deflections are recorded, providing an accurate reflection of the slab's structural behavior. Both the load at the first crack and the ultimate punching shear load, as well as their subsequent deflections at the slab center, were detected and recorded.

As seen in Fig. 10, a solid square steel cube with dimensions (40X40X40) mm was positioned over the middle of the slab to provide concentrated load.

Fig. 10 Punching Shear Test of Specimens

III. RESULTS AND DISCUSSION

3.1 Cracking and Ultimate Load

The main objective of this study is to determine the ultimate load capacity of reinforced concrete bubbled slab for punching shear because ultimate load is an important factor that makes indication of structural behavior. The observed failure loads of the tested slabs for each group are as bellow:

3.1.1 Group-one (Normal Strength Concrete)

This group is consisting of five normal Strength concrete specimens' slab with (30) MPa fć. First one is reference slab which was tested without expositing to fire and the four other specimens were burned to 300 C° and cooled in air, spraying water for 5 and 10 min and by using quenching in water for 10 min.

The tests show that the ultimate punching shear load for specimen NSC-R is (28) kN and the first crack appears at (10) kN which is (35.71 %) of the ultimate load. After burn other slabs NSC-A the one which cooled with air failed at (23) kN which is (17.9) % of the ultimate load for reference slab because of the heat effect on tension face of the concrete slab and the first crack appear at (7.5) kN which is lower than that in reference slab by (25) % and for the same reason. The results are comparable to those of Al-Gasham [13]. The cement paste expands when heated, but from 300ºC, a contraction occurs, associated with water loss. At this stage, aggregates continue to expand, and the resulting internal stresses can lead to loss of strength, cracking and flaking.

By moving to water cooling method spraying water on tension face for 5 and 10 min bring the load of specimen NSC-W5 and NSC-W10 down to (21 and 20) kN which is lower than that in control slab at (25 and 28.6) % and first crack appears at (6.5 and 6) kN which is less than the reference at (35 and 40) % and the reason of that decrease in ultimate load and first crack load is the fast and deeper deterioration caused by water and the effect of sudden cooling is show clearly in the last cooling method which is quenching the burned slab into water tank for 10 min and that made the ultimate load of NSC-Q decrease to (33.9) % of the ultimate load for reference slab at (18.5) kN and the first crack is (50) % from first crack load of the reference slab at (5) kN. First crack load varies from (27 to 35.71) % from the ultimate load of each specimen. The results in our study are close to what was observed by Botte and Caspeele [14] in their research where quenching the specimens after heating results in the highest possible strength loss compared to spraying water and cooled the specimens gradually and that loss could reach 38% for 350 C° of heating. Annerel [15] and Bingöl et al. [16] showed the same results and this reduction is mainly attributed to the formation of microcracks caused by high thermal stress. Table 2 and Fig. 11 show the results of this group.

Table 2 Ultimate Load Test Results for Group-One

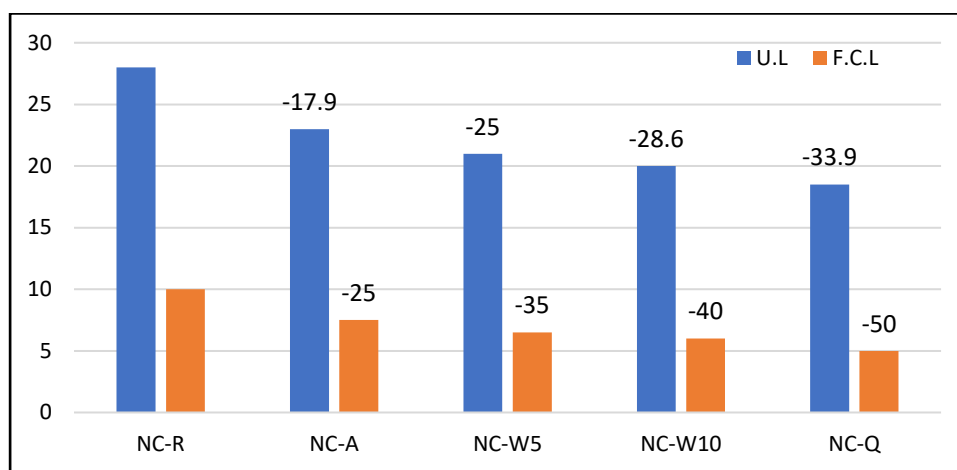| Groupname	Labeling	First Crack load(F.C.L) (kN)	Ultimate load (U.L) (kN)	$\dfrac{F.C.L}{U.L}$ (%)	$\dfrac{F.C.L}{(F.C.L)R}$ (%)	$\dfrac{U.L}{(U.L)R}$%
	NSC-R	10	28	35.71		
	NSC-Air	7.5	23	32.6	-25	-17.9
G1	NSC-W5	6.5	21	30.95	-35	-25
	NSC-W10	6	20	30	-40	-28.6
	NSC-Q	5	18.5	27	-50	-33.9

Fig. 11 Ultimate Load Results for Normal Strength Concrete

3.1.2 Group-two (0.5% Glass Fiber Concrete)

This set similarly consists of five specimens, but they are composed of (30) MPa of normal strength concrete reinforced with 0.5 % polypropylene reinforced glass fiber.

Polypropylene (PP) fiber was added into the slab to avoid explosive spalling of the concrete and to regulate the temperature rise in the steel mesh during a fire, this increased the fire resistance of the concrete [17]. The reference specimen GF0.5-R fails at a load of (29.5) kN, which is (5) % greater than the NSC-R specimen, and the first crack appears at a load of (12.5) kN, which is (42.3) % of the ultimate load. After burn slab GF0.5-A and test after let it cool in room temperature the specimen failed at (25) kN, which is (-11.9) % of the ultimate load of the reference slab GF0.5-R and the first crack appeared at (10.75) kN, which is less than that in reference slab at (-14) %. In comparison to the non-fiber specimen NSC-A, which was also burned and cooled to room temperature, the ultimate punching shear strength and initial cracking load were significantly reduced from (-17.9) % to (-11.9) %. As the numbers indicate, the strength and stiffness of the specimen without fiber significantly reduces following the fire test, despite the fact that the plastic performances remain comparable. This phenomenon could be a result of explosive spalling or the excessive steel mesh heating effect. However, no such considerable loss of strength or stiffness is observed in specimens reinforced with PP fiber, independent of the fiber amount [18].

By advancing to the water-cooling method, spraying water on tension face for 5 and 10 min bring the ultimate load of GF0.5-W5 and GF0.5-W10 down to (23.5 and 22) kN which is lower than that in control slab GF0.5-R at (-20.3 and -25.4) % and first crack show at (8.7 and 7) kN which is less than the

reference slab first crack at (-30.4 and -44) %. The explanation for the significant decrease in ultimate punching load capacity when specimens are cooled with water is that when fibers melt at around 170 ℃, microstructural waterways form in the slab, allowing water to permeate deeper into the slab body, resulting in increased deterioration. [19].

The influence of water cooling is obvious in the final cooling technique which is quenching the burned slab into water for 10 min and that made the ultimate load of GF0.5-Q decrease to (-32.2) % of the reference slab GF0.5-R at (20) kN and the first crack is (-52) % from first crack load of the reference slab at (6) kN. The results in details as in Table 3.

The addition of glass fibers improves the mechanical characteristics, which accounts for the rise in ultimate shear force capacity by (5) % comparing to normal strength concrete specimens. Additionally, the fibers act as a barrier to microcracks in concrete, which explains why the first crack load increases to reach (42.3) % of ultimate load in GF0.5-R but that's increase evanesce by using water to cool the specimens because adding glass fiber to concrete increase the porosity of concrete making water penetrates slab surface deeper than other slabs causing more deterioration. Additionally, the fibers help reduces spalling in concrete by creating channels for trapped moisture to escape after they are burned at a temperature of 170 ℃. The fig.12 Illustrates the numbers graphically.

Table 3 Ultimate Load test results for 0.5% Glass Fiber Concrete

Group name	Labeling	First Crack load (F.C.L) (kN)	Ultimate load (U.L) (kN)	$\dfrac{F.C.L}{U.L}$ (%)	$\dfrac{F.C.L}{(F.C.L)R}$ (%)	$\dfrac{U.L}{(U.L)R}$ %
G2	GF0.5-R	12.5	29.5	42.3		
	GF0.5-A	10.75	26	41	-14	-11.9
	GF0.5-W5	8.7	23.5	37	-30.4	-20.3
	GF0.5-W10	7	22	31.8	-44	-25.4
	GF0.5-Q	6	20	30	-52	-32.2
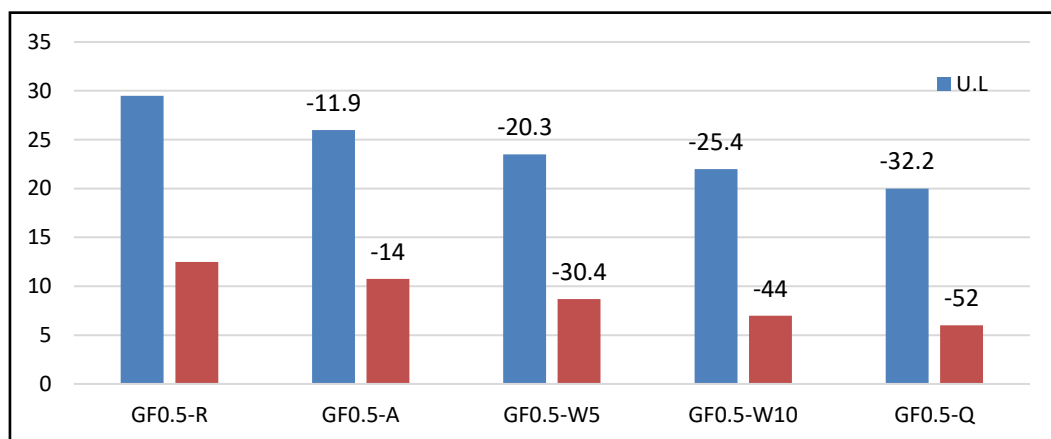
Fig. 12 Ultimate Load results for 0.5% Glass Fiber Concrete

3.1.3 Group-Three (1.0% Glass Fiber Concrete)

As with the previous group, this one uses the same number of slabs and the same test technique but, the fiber content is raised to 1%.

The reference specimen GF1.0-R fails at a load of (27) kN, which is (3.58) % less than the reference normal strength concrete NSC-R specimen, and the first crack appears at a load of (10) kN, which is (37) % of the ultimate load. By increasing the percentage of fibers to 1%, it is clear that the overall mechanical properties of the concrete have deteriorated by 3.57 % and 8.5 %, respectively, when compared to normal and 0.5 %

glass fiber concrete, because the addition of fibers increases the air content in the concrete, making it weaker and losing its advantage of restricting cracks in the structure of slabs, so that first crack load is degrading. All of this degrades back to the optimum dosage of polypropylene fiber, which is the proportion of fibers where we get the best results, which is often about 0.25-0.5 percent [20]. Thus, at a glass fiber content of 0.5 percent, close to that ideal percentage, but as the glass fiber content increased to 1.0 percent, we retreated from it. Without stating the optimum proportion in our study, as this is not our primary interest.

After burn slab GF1.0-A and test after let it cool in room temperature the specimen failed at (21) kN, which is (-22) % of the ultimate load of the reference slab GF1.0-R. the higher the fiber content, the worse the slab degrades, as seen in slab GF1.0-A., and the first crack appeared at (7.5) kN, which is less than that in reference slab at (-25) %.

As in 0.5 Glass fiber group the effect of water cooling was clearly obvious in term of ultimate punching shear strength of the specimens so that spraying water on tension face for 5 and 10 min bring the ultimate load of GF1.0-W5 and GF1.0-W10 down to (19.5 and 18.5) kN which is lower than that in control slab GF1.0-R at (-27.8 and -31.5) % and first crack show at (6.5 and 5.5) kN which is less than the reference slab first crack at (-35 and -45) %. Quenching the burned slab into water for 10 min made the ultimate load of GF1.0-Q decrease to (-41) % of the reference slab at (16) kN and the first crack is (-55) % from first crack load of the reference slab at (4.6) kN. The results in details as in Table 4.

By increasing the percentage of fibers to 1%, it is clear that the overall mechanical properties of the concrete have deteriorated by 3.57 % and 8.5 %, respectively, when compared to normal and 0.5 % glass fiber concrete group, because the addition of fibers increases the air content in the concrete, making it weaker and losing its advantage of restricting cracks in the structure of slabs and the fibers creating channels after they are melting at a temperature of 170 °C. Another significant effect of higher fiber dosage is the full elimination of spalling, as moisture seeks for additional pathways to escape before spalling starts.

Table 4 Ultimate Load test results for 1.0% Glass Fiber Concrete

Group Name	Labeling	First Crack load (F.C.L) (kN)	Ultimate load (U.L) (kN)	$\dfrac{F.C.L}{U.L}$ (%)	$\dfrac{F.C.L}{(F.C.L)R}$ (%)	$\dfrac{U.L}{(U.L)R}$ %
G3	GF1.0-R	10	27	37		
	GF1.0-A	7.5	21	35.7	-25	-22
	GF1.0-W5	6.5	19.5	33.34	-35	-27.8
	GF1.0-W10	5.5	18.5	29.7	-45	-31.5
	GF1.0-Q	4.5	16	28.1	-55	-41

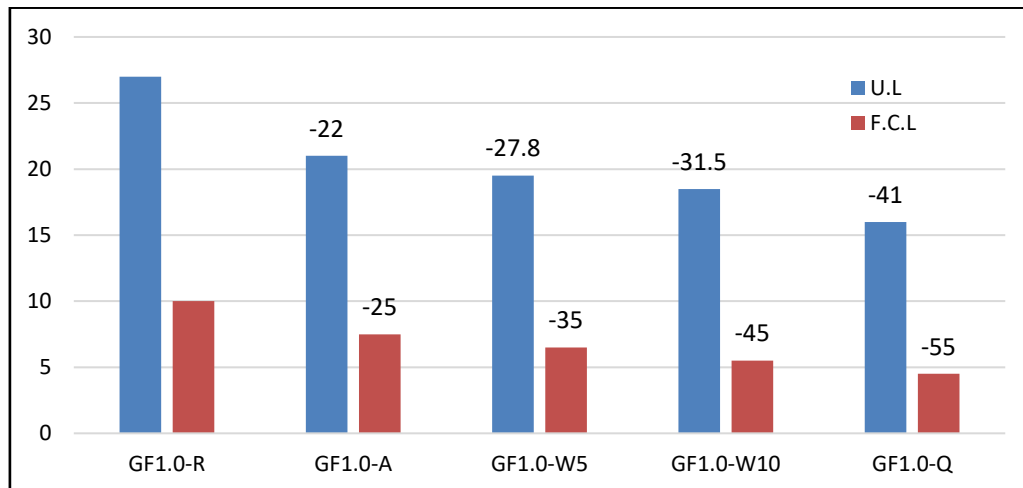Fig.13 show the variation in ultimate punching shear load in different cooling method.

Fig. 13 Ultimate Load results for 1.0% Glass Fiber Concrete

3.2 Load-Deflection relationship

The deflection was measured at the center of slabs using a (0.01mm) dial gage with a load increment of 2.5 kN, and readings for these gages were recorded for each load increment. When a reinforced concrete slab is gradually loaded, the deflection increases linearly in an elastic manner. Once cracks begin to form, the slab's deflection increases at a faster rate. After the slab develops cracks, the load-deflection curve is nearly linear until the flexural reinforcement begins to yield, at which point the deflection continues to increase without an appreciable increase in load. Fig. 14 illustrate the load-deflection relationship for all specimens.

Polypropylene (glass) fiber is well-known for its enhancing properties when added toconcrete, particularly in high-temperature scenarios because its resistance to spalling, and other primary application is to resist cracking during the first stage of loading and subsequent phases and this definitely has an effect on the deflection value and load-deflection curves that result.

The reference specimen GF0.5-R exhibits greater resistance to deflection in both the first crack load and ultimate load tests than the NSC-R specimen. Even after burning, the resultant deflection is still less than that of normal concrete specimens, despite the fact that the fibers melt during the early stages of fire exposure. However, this decreases spalling rate in the concrete cover, making the slabs stronger.

Increased glass fiber content to 1% reduces the overall mechanical properties of concrete, including deflection. Even when not exposed to fire, reference specimen GF1.0-R exhibits greater deflection than NC-R, but fire has a massive impact on other specimens.Water cooling degrades the concrete structure more than air cooling, particularly the quenching approach, where the large porosity of the concrete structure resulted in a significant loss of stiffness.

Fig. 14 illustrate the load-deflection relationship for all specimens.Table 5, 6 and 7 show Deflection's value.
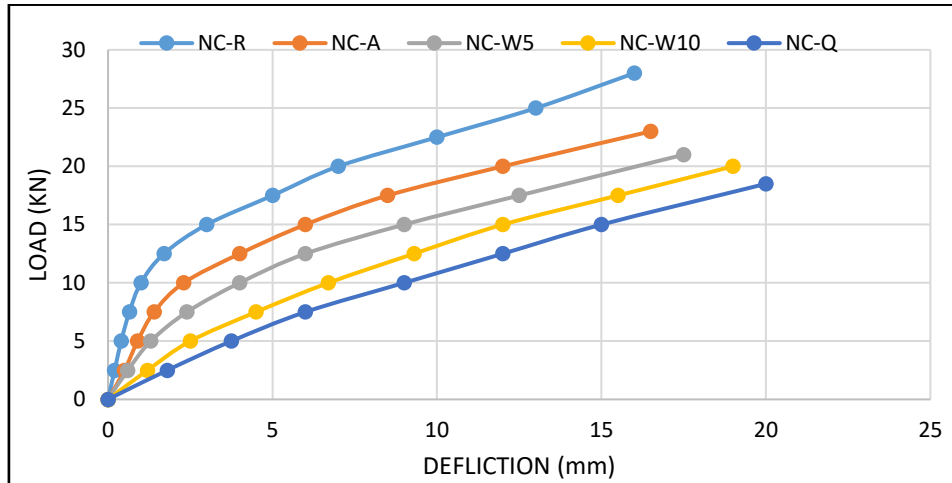
(a) Load-Deflection Curves of Normal Strength Concrete Group
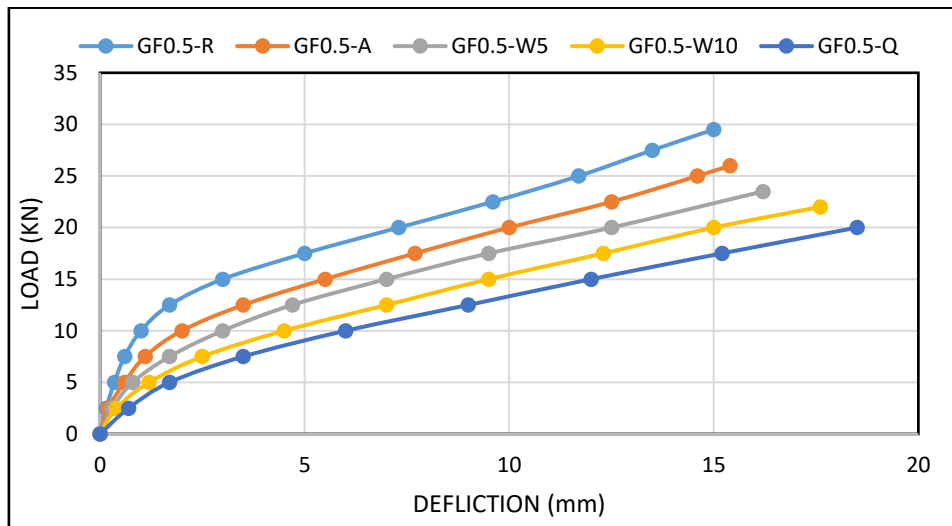
(b) Load-Deflection Curves Of (0.5 %) Glass Fiber Concrete Group
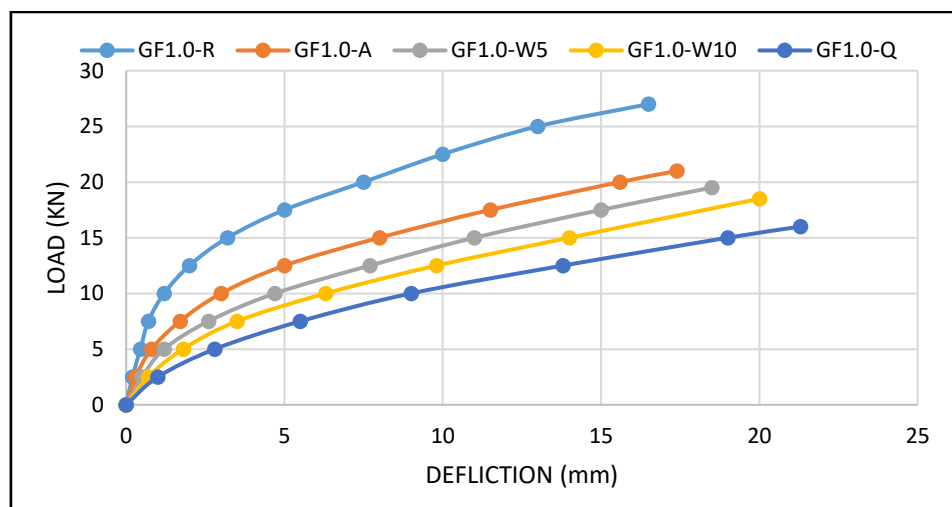
(c) Load-Deflection Curves Of (1.0 %) Glass Fiber Concrete Group

Fig. 14 Load-Deflection Curve

Table 5 Normal Strength Concrete Slabs Deflections

Group No.	Specimens	U.L (kN)	Deflection at U.L (mm)	Percentage of increase (%)
G1	NSC-R	28	16	
	NSC-A	23	16.5	3.1
	NSC-W5	21	17.5	9.4
	NSC-W10	20	19	18.75
	NSC-Q	18.5	20	25

Table 6 (0.5 %) Glass Fiber Concrete Deflections

Group No.	Specimens	U.L (KN)	Deflection at U.L (mm)	Percentage of increase (%)
G2	GF0.5-R	29.5	15	
	GF0.5-A	26	15.4	2.7
	GF0.5-W5	23.5	16.2	8
	GF0.5-W10	22	17.6	17.4
	GF0.5-Q	20	18.5	23.3

Table 7 (1.0 %) Glass Fiber Concrete Deflections

Group No.	Specimens	U.L (KN)	Deflection at U.L (mm)	Percentage of increase (%)
G3	GF1.0-R	27	16.5	
	GF1.0-A	21	17.4	5.5
	GF1.0-W5	19.5	18.5	12.1
	GF1.0-W10	18.5	20	21.2
	GF1.0-Q	16	21.3	29

3.3 Crack Pattern and Punching Zone perimeter

Fig. 15 indicates the punching shear behavior associated to simply supported reinforced concrete slabs which are exposed to fire from beneath. The slabs' ends can rotate freely, also the slab can elongate freely (thermally un-restrained). Glassfibers contains straight bars which are positioned close to slab's bottom. As the slab's underside is exposed to fire, bottom will be expanding more than top, the subsequent curvature makes the slab deflecting downwards. In the case when the reinforcement's strength decreases less than that needed for supporting slabs and any superposed load, the punching or flexural and punching failure is going to occur [13].
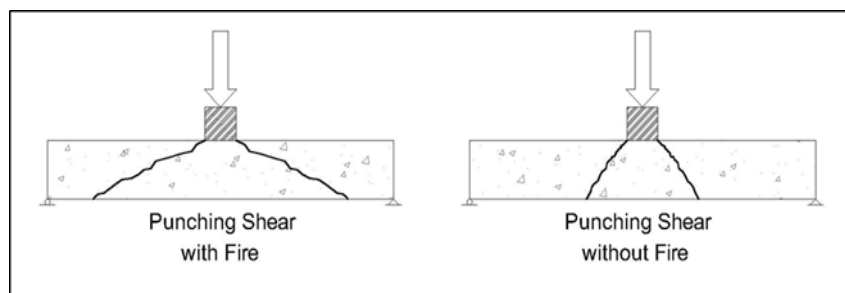
Fig. 15 The Impact of Fire on punching shear of Simply Supported Reinforced Concrete Slab.

The difference in crack pattern between Glass fibers bubble slabs and normal strength concrete slabs was clearly shown due to the nature of the two materials, with glass fiber specimens being tougher as shown in fig. 16, 17 and 18.
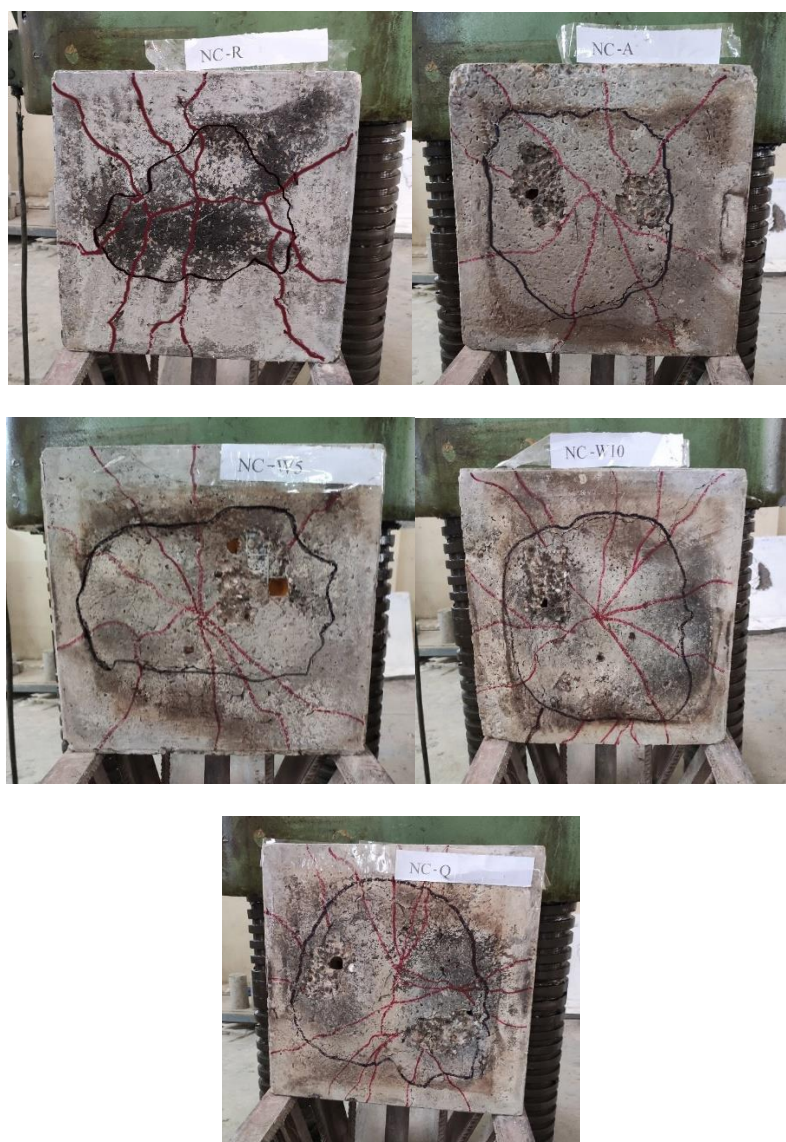
Fig. 16 crack pattern and punching perimeters of normal strength concrete
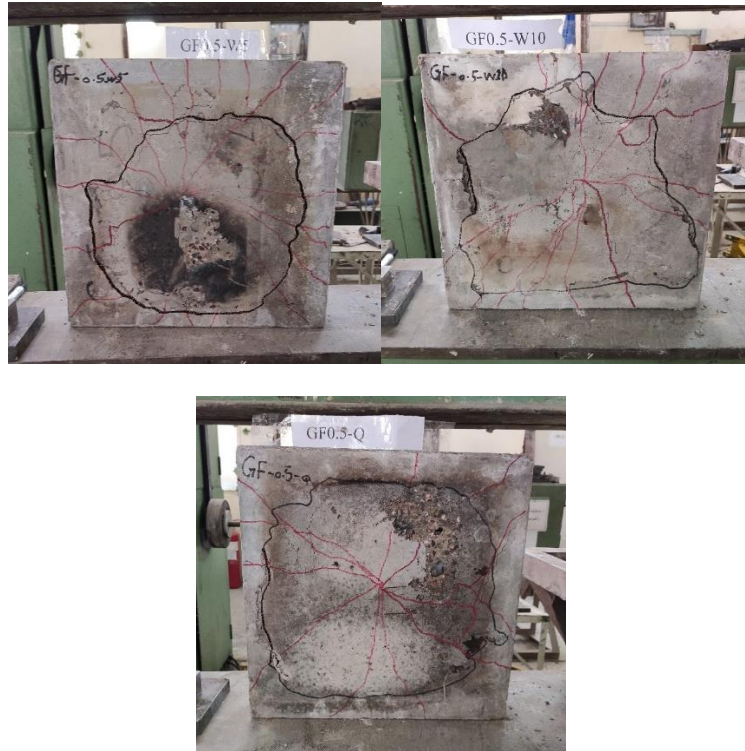
Fig. 17 Crack Pattern and Punching Perimeters of 0.5% Glass Fiber Concrete
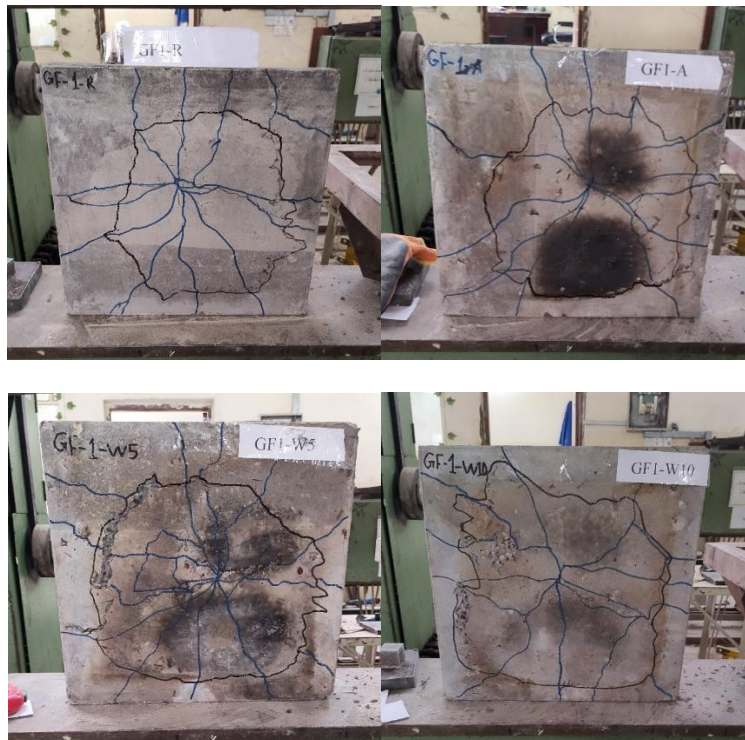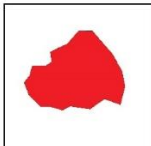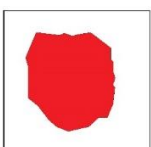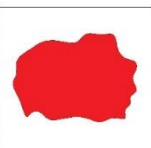
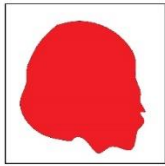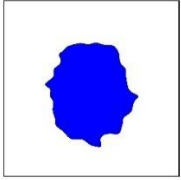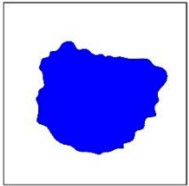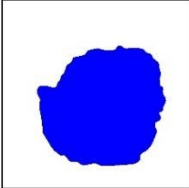Fig.18 Crack Pattern and Punching Perimeters of 1.0 % Glass Fiber Concrete
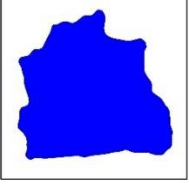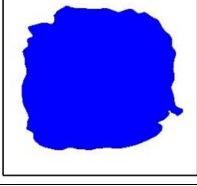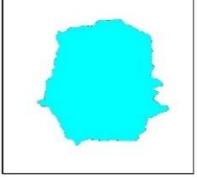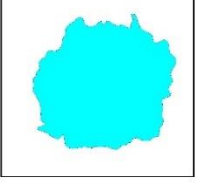
Punching zone was measured using Auto CAD by exporting a clear straight image to the program and draw over the punching area and using the command Area to calculate the actual area. the punching zone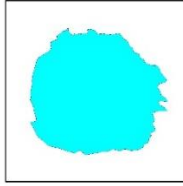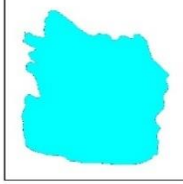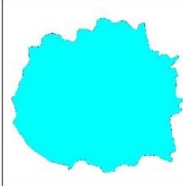 perimeter give an indicate of specimen strength at punching shear test and that is clear in the results, where in references specimen was the smaller and with air cooled one it was bigger and it continue to be bigger in water cooling slab and that show the real effect of fire on concrete.

Table 8 show the punching area for each specimen.

Table 8 Punching Zone Perimeters

Specimen	Perimeter Measured by Auto Cad (m)	Measured Area (m^2) by Auto Cad	$\frac{Punching\ Area}{Total\ Area}$(%)	Zone of Failure
NSC-R	0.9064	0.0488	24.1	
NSC-A	0.9844	0.0677	33.4	
NSC-W5	1.0725	0.0711	35.1	
NSC-W10	1.1466	0.0945	46.7	

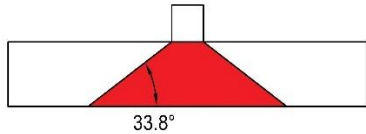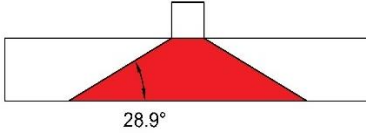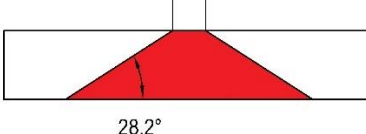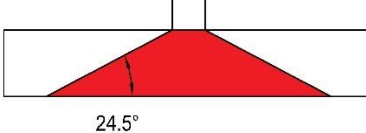|			
NSC-Q	1.2075	0.0983	48.5	
GF0.5-R	0.83	0.8335	0.0433	
GF0.5-A	1.02	1.0243	0.0631	
GF0.5-W5	1.03	1.0125	0.0672	
GF0.5-W10	1.33	1.3278	0.0967	
GF0.5-Q	1.3	1.3048	0.1022	
GF1.0-R	1.1	1.1015	0.0627	
GF1.0-A	1.25	1.2394	0.0782	

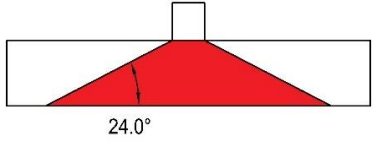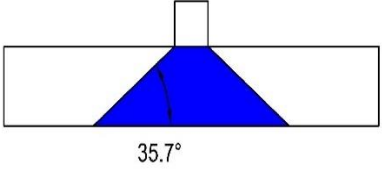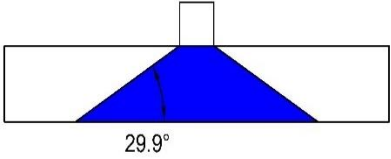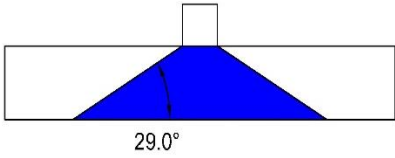|				
GF1.0-W5	1.22	1.2317	0.0817	
GF1.0-W10	1.5	1.4994	0.1040	
GF1.0-Q	1.56	1.5596	0.1108	
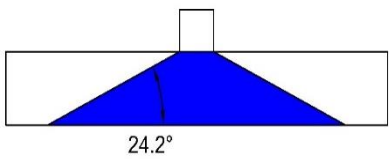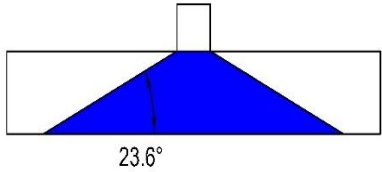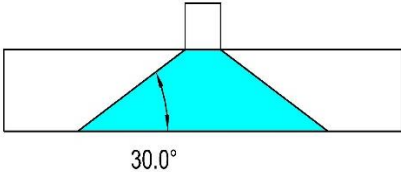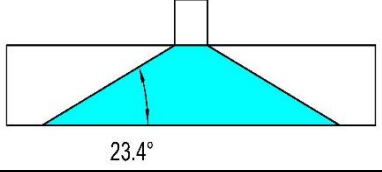
3.4 Angle of Failure
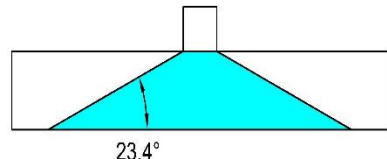
Typically, the punching failure mode was formed like a conical pyramid, with the specimens' bottom faces at a (Ø) angle. The punching zone assumed to be circular, with a circular punching zone and a specified perimeter, the radius of the assumed circle can be determined using the circle area equation. Following that, AutoCAD was used to determine the angle of failure for all specimens as shown in Table 9. The angle of failure gave an indicate to the strength of specimens where stronger specimen has bigger failure angle [21]. Experimental work show that all reference slabs have bigger failure angle than that in other slab in the same group and for all group cooling specimens gradually in air have lower impact on angle of failure in opposite to water cooling where specimens tend to have smaller failure angle.

Table 9 Angle of Failure for all specimens
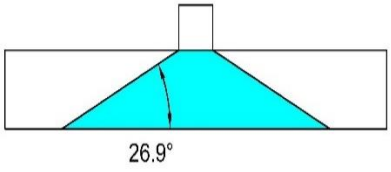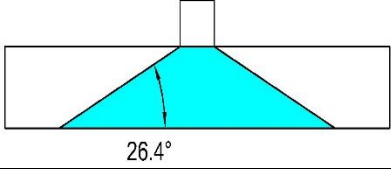
Specimen	Area measured by AutoCAD (m²)	Radius (m)	Angle (θ°)	Angle of Failure
NSC-R	0.0488	0.1246	34.8º	 33.8°
NSC-A	0.0677	0.1468	29.9º	 28.9°
NSC-W5	0.0711	0.1504	28.2º	 28.2°
NSC-W10	0.0945	0.1734	25.5º	 24.5°

NSC-Q	0.0983	0.1769	24º	24.0°
GF0.5-R	0.0433	0.1174	35.7º	35.7°
GF0.5-A	0.0631	0.1417	29.9º	29.9°
GF0.5-W5	0.0672	0.1463	29º	29.0°
GF0.5-W10	0.0967	0.1754	24.2º	24.2°
GF0.5-Q	0.1022	0.1804	23.6º	23.6°
GF1.0-R	0.0627	0.1413	30º	30.0°
GF1.0-A	0.0782	0.1578	26.9º	26.9°
GF1.0-W5	0.0817	0.1613	26.4º	26.4°
GF1.0-W10	0.1040	0.1819	23.4º	23.4°

GF1.0-Q	0.1108	0.1878	23.4°	

3.5 Critical Section Perimeters

In accordance with ACI (318-19) [22] and B.S. (8110) [23] the critical section perimeter was assumed to be at (d/2) and (1.5d) from the column face. For the slabs examined in this study, the critical section is defined as half the distance between the end of the failure surface and the column side. The computed distances are based on the area of failure measured using AutoCAD. The technique for calculating the critical sections for the investigated slabs is shown in Figure (19). Tuan [24] demonstrated that the critical section perimeters for high strength concrete are equal to (2d), which is consistent with (CEB-FIP Model Code-1990) [25]. Table (10) contains the estimated critical section values for each set of slabs tested.
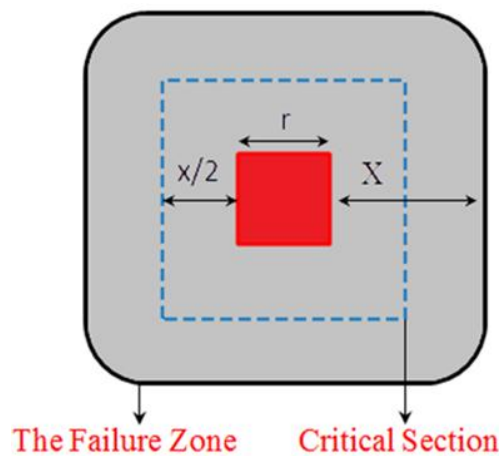
Fig. 19 Calculation of Critical Sections

$$\pi x^2 + 4rx + r^2 = A$$

$$(r^2 - A) + 4r\,x + \pi x^2 = 0$$

$$X = \frac{\sqrt{(4r)^2 - 4\pi(r^2 - A)} + (-4r)}{\pi * 2}$$

Where:

A: is the area of punching (m²).
r: Square column side length (m).
x: distance between the end of the failure zone and the column's side (m).

Table 10 distance of critical section from face of column

Specimen	Area measured by Auto Cad (m²)	X (m)	Location of punching shear section from face of column			
			Measured X/2 (m)	ACI 318 d/2 (m)	BS8110 1.5d (m)	CEB-FIP-MC-90 2d (m)
NSC-R	0.0488	0.0997	0.0499	0.02	0.06	0.8
NSC-A	0.0677	0.1218	0.0609	0.02	0.06	0.8
NSC-W5	0.0711	0.1254	0.0627	0.02	0.06	0.8
NSC-W10	0.0945	0.1484	0.0742	0.02	0.06	0.8
NSC-Q	0.0983	0.1518	0.0759	0.02	0.06	0.8

GF0.5-R	0.0433	0.0925	0.0463	0.02	0.06	0.8
GF0.5-A	0.0631	0.1167	0.0584	0.02	0.06	0.8
GF0.5-W5	0.0672	0.1213	0.0606	0.02	0.06	0.8
GF0.5-W10	0.0967	0.1504	0.0752	0.02	0.06	0.8
GF0.5-Q	0.1022	0.1553	0.0776	0.02	0.06	0.8
GF1.0-R	0.0627	0.1163	0.0581	0.02	0.06	0.8
GF1.0-A	0.0782	0.1327	0.0664	0.02	0.06	0.8
GF1.0-W5	0.0817	0.1362	0.0681	0.02	0.06	0.8
GF1.0-W10	0.1040	0.1569	0.0784	0.02	0.06	0.8
GF1.0-Q	0.1108	0.1627	0.0814	0.02	0.06	0.8

IV. CONCLUSION

The following conclusions are being made from the experimental results obtained in this study:

1. When RC bubbled slabs are exposed to a fire flame and reach a temperature of 300 °C for 30 minutes, the ultimate punching shear strength of the slabs significantly decreases and deflection increases due to the loss of stiffness.

2. Because of concrete can slowly recover during cooling, gradually air cooling has a smaller influence on all mechanical properties (punching shear strength, deflection, failure zone, angel of failure) for slabs following a fire test.

3. Spraying water onto the tension face of slabs for five minutes create a thermal shock that had a significantly greater effect on the mechanical properties of concrete than air cooling, but was significantly less than quenched and ten-minute water spraying.

4. The effect of a ten-minute water spray is comparable to the effect of a quenching treatment on slabs where the concrete has deteriorated significantly and was unable to recover from the fire flame effect.

5. The "real" effect of water cooling became apparent when quenching was used to cool burned slabs when the punching shear strength was reduced and the deflection was more than with other cooling methods, but as close as 10 minutes water spraying.

6. 6.Spalling was the primary cause of increased punching shear strength losses.

7. Our test discovered that glass fiber (Polypropylene fibers) is a double-edged sword, as there is a specific glass fiber content that significantly improves all mechanical properties of concrete, while adding even a small amount above that proportion degrades these properties, despite the complete elimination of spalling.

8. After cooling with water, glass fiber slabs or specimens exhibit a greater loss of strength and bigger failure zone.

9. 0.5 % glass fiber (Polypropylene fibers) content showed significant decrease in spalling rate, while 1.0 % glass fiber content led to complete elimination of spalling.

REFERENCES

[1.] J. Khalaf, Z. Huang, M. Fan. A Study About the Effect of Bond between Steel Reinforcement and Concrete Under Fire Conditions. *11th International Conference on Developments in eSystems Engineering (DeSE), Cambridge, United Kingdom, pp. 208-213,* 2018.

[2.] K. Cábová, L. Blesák, F. Wald. Advanced prediction methods in structural fire safety engineering. *Smart Cities Symposium Prague (SCSP), Prague, pp. 1-5*, 2016.

[3.] Chung et al., Flexural Capacities of Hollow Slab with Material Properties. *Proceedings of the Korea Concrete Institute, Vol.22, No.1, pp. 345- 350*, 2010.

[4.] ASTM E119-07a., Standard Test Methods for Fire Tests of Building Construction and Materials. ASTM International, West Conshohocken, PA, www.astm.org, 2007.

[5.] P. PrabhuTeja, P. Vijay Kumar, S. Anusha, C. Mounika and P. Saha, Structural behavior of bubble deck slab. *IEEE-International Conference on Advances in Engineering, Science and Management (ICAESM-2012), Nagapattinam, Tamil Nadu, pp. 383-388,*

2012.

[6.] Bubble Deck Voided Flat Slab Solution-Technical Manual and Documents. "Bubble Deck Span Properties". www.BubbleDeck.com.(2006).

[7.] AamerNajimabbas, Experimental Study of Polypropylene Fiber Reinforced Concrete Panels Subjected to Elevated Temperatures, *Journal of Engineering and Development, Vol. 14, No. 2*, 2010.

[8.] Ali A. Jaber, Ahlam S. Mohammed, Sura A. Abbas, Behavior and Strength of Polypropylene Reinforced Concrete Slabs, *Journal of Engineering Science and Technology, Vol. 16, No. 2 (2021) 1746 – 1760*.

[9.] Bubble Deck Voided Flat Slab Solution-Technical Manual and Documents. "Bubble Deck Span Guide". www.BubbleDeck.com.(2006).

[10.] ASTM A1064 / A1064M-18a, Standard Specification for Carbon-Steel Wire and Welded Wire Reinforcement, Plain and Deformed, for Concrete. ASTM International, West Conshohocken, PA, www.astm.org.(2018).

[11.] Mohammed M. H., Reinforced Concrete Strengthening by Using Geotextile Reinforcement for Foundations and Slabs. Master of Science in Civil Engineering, Civil Engineering Department, college of Engineering, Mustansiriyah University, 2017.

[12.] ASTM C31 / C31M-12, Standard Practice for Making and Curing Concrete Test Specimens in the Field. ASTM International, West Conshohocken, PA, www.astm.org. 2012.

[13.] Thaar Al-Gasham., Structural Performance of Reinforced Concrete Bubble Slabs after Exposing to Fire Flame. *Journal of Engineering and Development, 1919. 1813-7822*, 2015.

[14.] Wouter Botte, Robby Caspeele. post-cooling properties of concrete exposed to fire. Fire *Safety Journal 92, 142–150*, 2017.

[15.] E. Annerel, Assessment of the Residual Strength of Concrete Structures after Fire Exposure. PhD thesis, Ghent University.2010.

[16.] Bingöl, A. F., Gül, R., Effect of elevated temperatures and cooling regimes on normal strength concrete. *Fire and Materials, 33(2), 79–88*,2009.

[17.] Chul Hun Chung, Jungwhee Lee, Hyun Jun Kim, Evaluation of Fire Performance of Polypropylene Fiber RC Slabs, *KSCE Journal of Civil Engineering 17(5):1040-1050*, 2013.

[18.] Chul Hun Chung, Jungwhee Lee, Sun Hee Choi, Temperature Distribution Within Polypropylene Fiber-Mixed Reinforced Concrete Slabs Exposed to an ISO 834 Standard Fire, *KSCE Journal of Civil Engineering (0000) 00(0):1-9*, 2015.

[19.] Noumowe,Mechanical Properties and Microstructure of High Strength Concrete Containing Polypropylene Fibres Exposed to Temperatures Up to 200 ºC, *Cement and Concrete Research 35, 2192 – 2198*, 2005.

[20.] Anthony Nkem Ede, Optimal Polypropylene Fiber Content for Improved Compressive and Flexural Strength of Concrete, *IOSR Journal of Mechanical and Civil Engineering (IOSR-JMCE), Volume 11, Issue 3 Ver. IV (May- Jun. 2014), PP 129-135*.

[21.] Abeer H. Wenas. Structural Behavior of Embedded Collar Shear Head in Flat Plate with Opening, Master of Science in Civil Engineering, Civil Engineering Department, Faculty of Engineering, Mustansiriyah University, 2014.

[22.] ACI CODE 318-19. Building Code Requirements for Structural Concrete and Commentary. American Concrete Institute, Farmington Hill, MI.2019.

[23.] British Standards Institution (B.S.8110), Code of Practice for Design and Construction Part 1. London. (1997).

[24.] Tuan, N., Punching Shear Resistance of Reinforced Concrete Slabs. Electronic *Journal of Structural Engineering, Department of Civil and Environmental Engineering, The University of Melbourne, PP.5259*,2001.

[25.] CEB-FIP Model Code-1990, "Comité Euro-International Du Béton-Fédération de la Précontrainte", Model Code, Bulletin d'information, No.203-305, Lausanne, Switzerland,1990, 462pp.